Acta Scientiarum. Biological Sciences
ISSN: 1679-9283
ISSN: 1807-863X
actabiol@uem.br
Universidade Estadual de Maringá
Brasil

Santos, John Lenon de Souza; Câmara, Alice Barros;
Meira, Isabella Tanus Job e; Oliveira, Ivan Nobre

Study of comparative proteome between normal and inverted karyotypes of human mesenchymal stem cells

Acta Scientiarum. Biological Sciences, vol. 42, 2020, pp. 1-19
Universidade Estadual de Maringá
Maringá, Brasil

DOI: https://doi.org/10.4025/actascibiolsci.v42i1.50260

Acta Scientiarum

http://periodicos.uem.br/ojs/acta
ISSN on-line: 1807-863X
Doi: 10.4025/actascibiolsci.v42i1.50260

Study of comparative proteome between normal and inverted karyotypes of human mesenchymal stem cells

John Lenon de Souza Santos*, Alice Barros Câmara, Isabella Tanus Job e Meira and Jonas Ivan Nobre Oliveira

Departamento de Biofísica e Farmacologia, Centro de Biociências, Universidade Federal do Rio Grande do Norte, Av. Senador Salgado Filho, 3000, 59064-741, Candelária, Natal, Rio Grande do Norte, Brasil. *Author for correspondence. E-mail: johnlenons.santos@gmail.com

ABSTRACT. Multipotent mesenchymal stem cells have been expanded *in vitro* for cellular therapy in numerous clinical settings without standardized culture conditions or quality-control schemes. The *in vitro* expansion is necessary to obtain sufficient cells for clinical applications. However, the expansion may induce genetic and functional abnormalities which may affect the safety and functionality of MSC, especially the chromosomal stability. This study aimed to investigate the protein profile of umbilical cord-derived MSC with normal and inverted karyotypes after expansion in the laboratory. Mass spectrometry analysis was performed and the Bradford method, Scaffold software, String and Cytoscape databases were employed to measure and characterize the protein content of umbilical cord-derived MSC. Networks of protein interactions, hub and bottleneck proteins were identified by proteomics and systems biology approaches. We found that proteins related to cellular stress were super expressed in inverted karyotype cells. Moreover, a high expression of Serpine 1, RHOA, and CTSB was found in these cells, which are proteins related to cancer. The albumin and ubiquitin proteins have been associated with a positive prognosis in cancer and cellular stress, and were up- and down-regulated in normal karyotype cells, respectively. The results suggests that the paracentric inversion inv(3)(p25p13) induced some type of cellular stress and genetic instability in human mesenchymal stem cells. These analyses showed the importance of carrying out studies related to the genetic instability of human mesenchymal stem cells using the protein expression profile as a parameter.

Keywords: genetic instability; protein profile; umbilical cord; interaction network.

Received on October 7, 2019.
Accepted on January 17, 2020.

Introduction

Human umbilical cords (UCh) have been considered a biological risk residue after birth. However, UCh have been an interesting source of mesenchymal stem cells (MSC) for being disposable and accessible (Yun et al., 2016). Mesenchymal stem cells from the human umbilical cord (MSC-UCh) can be used without raising any ethical issue since these cells are a generally discarded extra-embryonic tissue. MSC-UCh have a multipotent differentiation, proliferate fast and have a close ontogenetic relationship with embryonic stem cells (He et al., 2016). Therefore, the UCh is an excellent source of MSC and can be used in regenerative medicine, for example.

Human MSC have been the subject of studies in the field of regenerative medicine and bioengineering because of their capacity for self-renewal and differentiation in other cell types. However, these cells need to be expanded in order to obtain a suitable number of cells used in treating diseases (Fan, Zhang, & Zhou, 2011). MSC expansion requires time, and during this time chromosomal alterations such as chromosomal inversions and modification of cell characteristics can occur. Chromosomal inversions may lead to genetic instability and increase the risk of producing abnormal gametes. Abnormal gametes can lead to unbalanced offspring, with duplications and deficiency of inverted chromosome segments (Vieira & Ferrari, 2013).

Paracentric inversions are balanced chromosomal rearrangements involving two breaks in the same chromosomal arm, followed by a 180° rotation of the chromosomal segment and its re-insertion. Paracentric inversions do not include the centromere. Most inversions have unique breakpoints and the inversion incidence in humans is rare, being estimated at 0.1-0.5 $1{,}000^{-1}$ in the population. Paracentric inversions have been described in all human chromosomes, but they are most common in chromosomes 1, 3, 5, 6, 7, 11, and 14 (Rigola et al., 2015).

Balanced paracentric inversions generally appear to be harmless. Balanced inversions are usually clinically asymptomatic because they do not involve a quantitative variation of the genetic material. However, infertility, spontaneous abortions and cognitive deficit have been reported in some patients with this type of inversion. On the other hand, cytogenetic molecular methods are necessary to detect or to rule out the presence of unbalanced chromosomal alterations, especially when dealing with MSC used in gene therapies (Rigola et al., 2015).

In a previous study, our group found a paracentric inversion in the short arm of chromosome 3 (3p25-26) in MSC isolated from one umbilical cord. In this context, studying the MSC-UCh proteins is relevant since these molecules are directly or indirectly responsible for controlling all or almost all biological processes (Barbosa et al., 2012). Proteomics studies the set of proteins in a descriptive and quantitative way, as well as how the protein levels vary in the population depending on the environment or interactions with other proteins (Valledor & Jorrín, 2011). The proteome is dynamic and changes according to the physiological status and cell differentiation phases (Barbosa et al., 2012). In a quantitative proteomic analysis, 463 surface proteins were found in MSC submitted to differentiation in osteoblasts (Foster et al., 2005). Furthermore, 1,001 surface proteins were found in another quantitative analysis using MSC from bone marrow (Lee et al., 2013). Finally, an experiment found 1664 proteins in MSC, as 607 proteins were obtained from bone marrow and 1052 proteins were obtained from the nerve tissue (Bryukhovetskiy et al., 2014).

Systems biology is a tool used to build protein-protein interaction networks in order to understand the interactions between these molecules. Systems biology enables constructing mathematical models, simulations, data processing techniques, and integrating information, thereby achieving a better understanding of the interactions between the living systems components and their biological processes (Mesquita, Jorge, Souza Junior, & Cassino, 2014). Therefore, systems biology was used in order to analyze the paracentric inversion in MSC-UCh at a protein level. Overall, this research aimed to analyze the protein expression profile of human MSC with normal and inverted (inv(3)(p25p13) karyotypes in order to characterize and compare these cells.

Material and methods

Isolation of MSC-UCh

This work was submitted and approved by the Ethics Committee of the *Universidade Federal do Rio Grande do Norte* (CEP/UFRN No. 044.0.051.000-07). Umbilical cord specimens were aseptically obtained by doctors after written informed consent was signed by mothers. The umbilical cord was maintained in PBS buffer in the Laboratory of Molecular and Genomic Biology of the *Universidade Federal do Rio Grande do Norte* (LBMG/UFRN). The UCh was washed with PBS buffer to remove excess blood and other contaminants. After this washing, the UCh was cannulated and a 0.5% solution of type IV collagenase was introduced for endothelium enzymatic breakdown (40 minutes, 37°C). After disaggregation, the reaction was inhibited by adding fetal bovine serum (FBS) into the UCh vein. The cell wall suspension was collected on a Petri dish, placed in tubes and centrifuged at 2,000 rpm for 10 min. The supernatant was discarded and the cells' pellet was suspended with DMEM-low glucose supplemented culture medium (20% FBS and 1% antibiotic). The cell solution was transferred to culture flasks, which were kept in an incubator (37 °C, 5% CO_2) for 48 hours in order for the cells to adhere to the vials.

MSC characterization

The cell solution was sent to the Laboratory of Immunogenetics - Department of Biochemistry in the *Universidade Federal do Rio Grande do Norte* for flow cytometry by a FACSCanto II, BD cytometer. We performed flow cytometry and osteogenic, chondrogenic and adipogenic differentiation in order to characterize the cells as MSC. MSC are generally positive for CD105, CD90, and CD73 surface markers and negative for HLA-DR, CD45, CD34, and CD14 surface markers. In addition, MSC are able to differentiate into osteoblasts, chondrocytes, and adipocytes. The differentiation can be observed by staining the cells. The osteoblasts are stained with Alizarin red; chondrocytes are stained with Alcian blue and adipocytes are stained with Oil red (Dominici et al., 2006). A beta-galactosidase test was performed in order to verify if the cells used were in the senescence process. It is possible to see if the cells express beta-galactosidase through cell staining (blue cells are senescent) (Shevchenko, Wilm, Vorm, & Mann, 1996).

Cell culture

We used six samples. A cell culture was performed in two MSC lines. These cells were cultured in alpha-MEM culture medium supplemented with 10% FBS, 1% antibiotic, and 1% glutamine until the culture was approximately 90% confluent. The culture was washed with PBS. The cell pellet was dissolved in a lysis buffer containing 7M urea, 2M thiourea, 4% CHAPS, 30mM Tris-HCl (pH 8.5), and 50mM DTT. The cell extract was resuspended, centrifuged for 20 minutes (4 °C at 12,000 RPM), and the supernatant (protein extract) was collected. The proteins were measured by the Bradford method.

Mass spectrometry and protein expression

The proteins were digested enzymatically (*In vitro* digestion protocol: Anal. Chem., 1996 68: 850-858) and separated for mass spectrometry analysis. The protein extract was sent to the Mass Spectrometry Laboratory of the National Laboratory of Biosciences (CNPEM-ABTLuS) in the *Universidade de Campinas* (UNICAMP) for mass spectrometry analysis by Q-Tof spectrometer.

Scaffold software (http://www.proteomesoftware.com/products/scaffold/) was used to quantify and classify the proteins according to their profile (Scaffold Elements, version 2.1.1). The raw data from mass spectrometry were processed using Scaffold software, and the Fold Change value was obtained. The Fold Change value was used to classify the proteins as up-regulated and down regulated. In this context, we evaluated the proteins up-regulated and down-regulated expressed in cells with a normal karyotype, in cells with an inverted karyotype, and in both cell types.

Protein functions

The protein identification numbers (ID) generated by Scaffold software were converted into identification numbers compatible with the String database through the UniProt ID conversion tool (http://www.uniprot.org/uploadlists/). We then obtained six protein lists using Scaffold, including up-regulated proteins and down-regulated proteins of normal karyotype cells, and up-regulated proteins and down-regulated proteins of inverted karyotype cells. The lists were imported into the String database, which provided the molecular functions (MFs) and biological processes (BPs) of proteins (http://string-db.org/cgi/input.pl).

We analyzed the molecular functions (MFs) and biological processes (BPs) of down-regulated and up-regulated proteins of normal karyotype cells. These same steps were repeated for inverted karyotype cells. The REVIGO tool (http://revigo.irb.hr/) was used to review the protein categories in order to verify the absence of redundant categories. Finally, the networks generated in String database were exported to Cytoscape software (http://www.cytoscape.org/) to identify the measure of centrality or betweenness. The betweenness represents the number of shortest paths that pass through the protein. With the betweenness value, we can suggest what might be the hubs of the networks (highly connected proteins).

Results

No surface markers have been exclusively associated with MSC to date. Based on a proposal by the International Society for Cell Therapy, cells may be classified as MSC if they adhere to plastic, carry a minimal subset of characteristic surface markers (CD73, CD90, CD105) and present the potential to differentiate into bone, fat, and cartilage (Dominici et al., 2006). The cells isolated from the UCh vein were positive for CD105, CD90, and CD73 surface markers, and negative for HLA-DR, CD45, CD34, and CD14 surface markers. The cells were also able to differentiate into the three well-defined cell types: osteoblasts, chondrocytes, and adipocytes (Figure 1). Therefore, the analyzed cells are MSC.

Analysis of protein functions

Q-Tof spectrometry identified 321 expressed proteins, 15 were only expressed in Inverted karyotype cells (Table S1), 42 were only expressed in Normal karyotype cells (Table S2) and 264 were expressed in both cell types (TableS 3). In addition, regarding the 264 intersection proteins, 156 proteins were sub expressed and 91 proteins were super expressed in inverted karyotype cells compared to normal karyotype cells.

We analyzed 12 BP and 18 MF overall, where 8 BP were present in normal karyotype cells and 4 BP were present in inverted karyotype cells. Furthermore, 15 MF were present in normal karyotype cells and 3 MF were present in inverted karyotype cells (Figure 2). When comparing inverted karyotype cells and normal karyotype cells, two main BPs were observed: cytoskeleton organization in inverted karyotype cells and

intracellular transport in normal karyotype cells (Figure 2a). We also found cytoskeleton constitution in inverted karyotype cells and RNA binding in normal karyotype cells when analyzing MFs (Figure 2b).

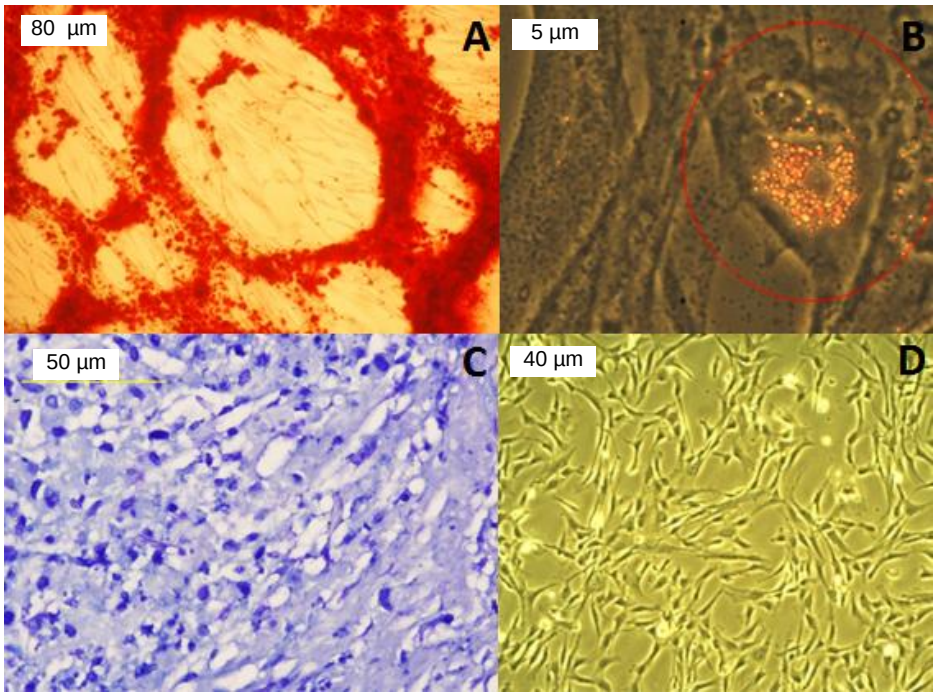

Figure 1. Types of cell differentiation. A) osteogenic: each gap corresponds to 1 mature osteocyte, which communicates with other osteocytes through communicating junctions (not visible); B) adipogenic: orange dots represent adipocytes, their color is derived from a large number of mitochondria and cytochrome oxidase available in the cytoplasm. Adipocyte size varies according to the number of lipid droplets present in the cytoplasm. C) chondrogenic: mature ovoid/rounded chondrocytes with basophilic cytoplasm and few organelles (not visible) in cartilaginous tissue gaps. D) cells without differentiation. Scale: A: 80 µm; B: 5 µm; C: 50 µm; D: 40 µm

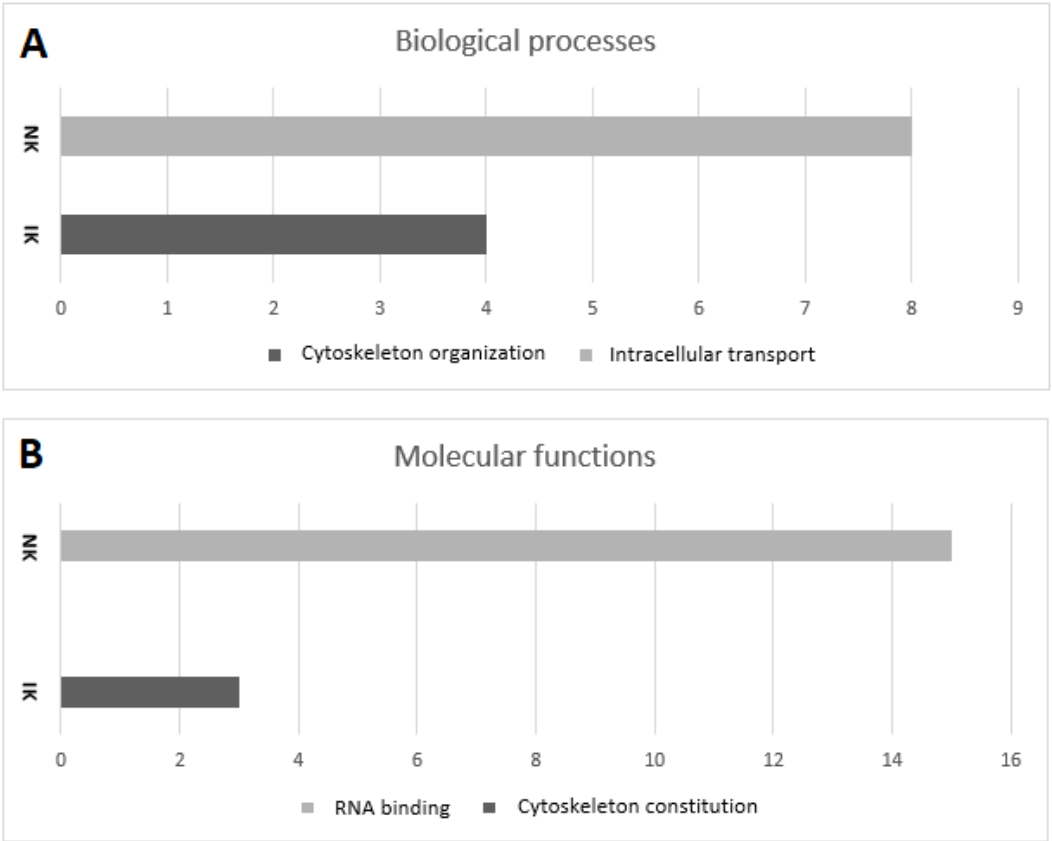

Figure 2. Distribution of the main biological processes (A) and molecular functions (B) in normal and inverted karyotype cells. IK, inverted karyotype; NK, normal karyotype.

Some general processes were observed when comparing the up-regulated proteins of normal karyotype cells and inverted karyotype cells and taking into consideration the BPs. We found proteins related to the negative regulation of BP, negative regulation of cellular processes, regulation of BP quality, regulation of apoptotic processes, response to stress, and response to the stimulus. These processes were only found in the inverted karyotype cells. In addition, the translation inhibition, regulation of cell death, tissue regeneration, response to tissue injury, and regulation of body fluids were processes which were only found in normal karyotype cells (Figure 3a).

General BP were also found when analyzing down-regulated proteins. Response to tissue injury, tissue regeneration, and binding proteins were BPs which were only found in inverted karyotype cells. Response to the stimulus, negative regulation of BP, regulation of body fluids, regulation of the immune system, and regulation of BP quality were only found in normal karyotype cells. Down-regulated proteins were related to 10 BPs, but only 2 BPs were common to inverted and normal karyotype cells: the negative regulation of cellular processes and the regulation of apoptotic processes. There is a greater amount of proteins related to these two processes in the inverted karyotype cells when compared to normal karyotype cells (Figure 3b).

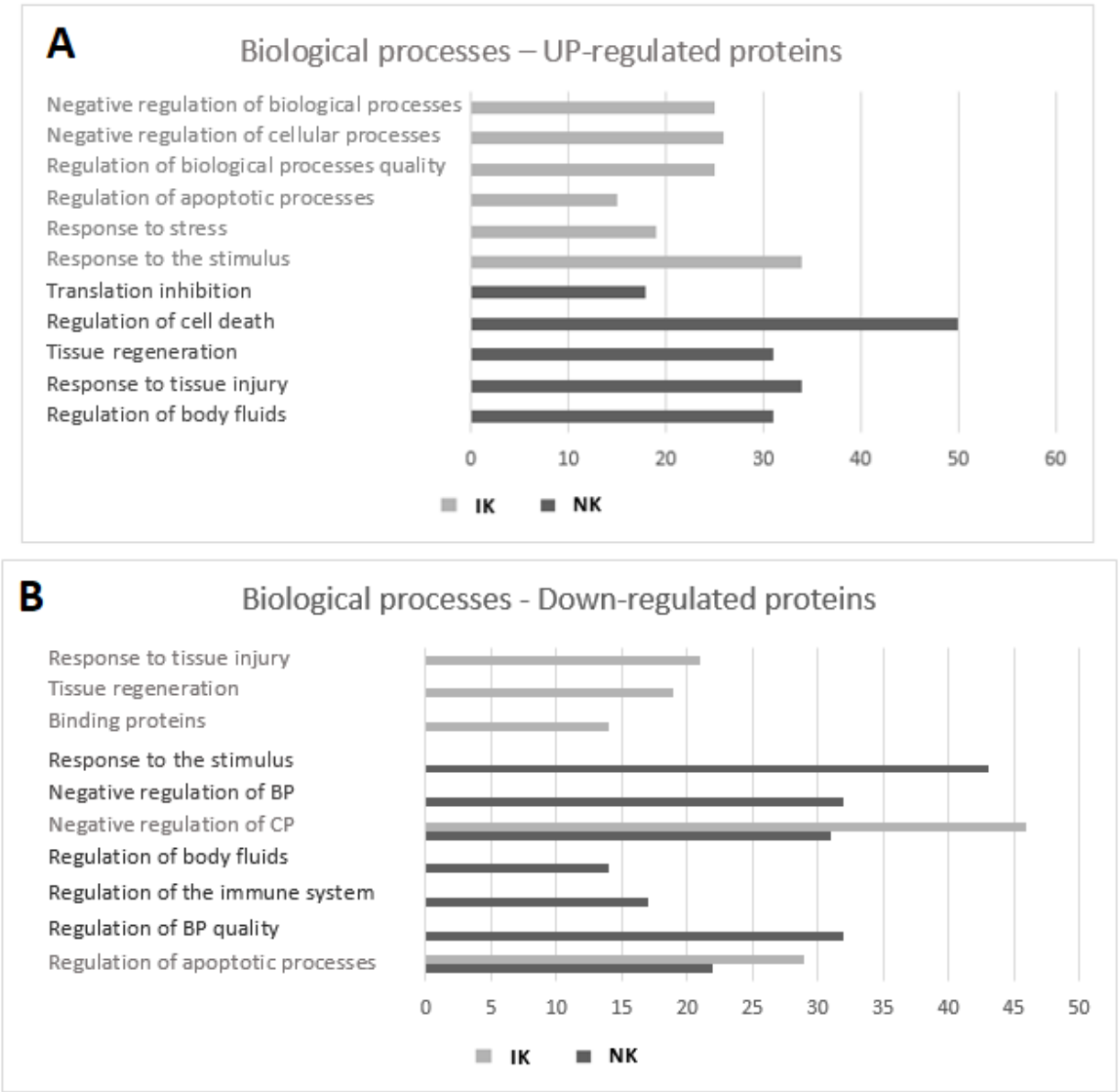

Figure 3. Quantification of up-regulated (A) and down-regulated (B) proteins related to each BP in normal and inverted karyotype cells. IK, inverted karyotype; NK, normal karyotype; BP, biological process; CP, cellular process.

Regarding the MFs of up-regulated proteins, the activation of structural molecules and cytoskeleton constitution were processes which were only found in inverted karyotype cells. In addition, a group of

binding enzymes was only found in normal karyotype cells. A greater amount of RNA binding proteins was also observed in normal karyotype cells when compared to the inverted karyotype cells (Figure 4a). Regarding the MFs of down-regulated proteins, the activation of structural molecules was only observed in normal karyotype cells. Additionally, a greater amount of RNA binding proteins was observed in inverted karyotype cells when compared to normal karyotype cells (Figure 4b).

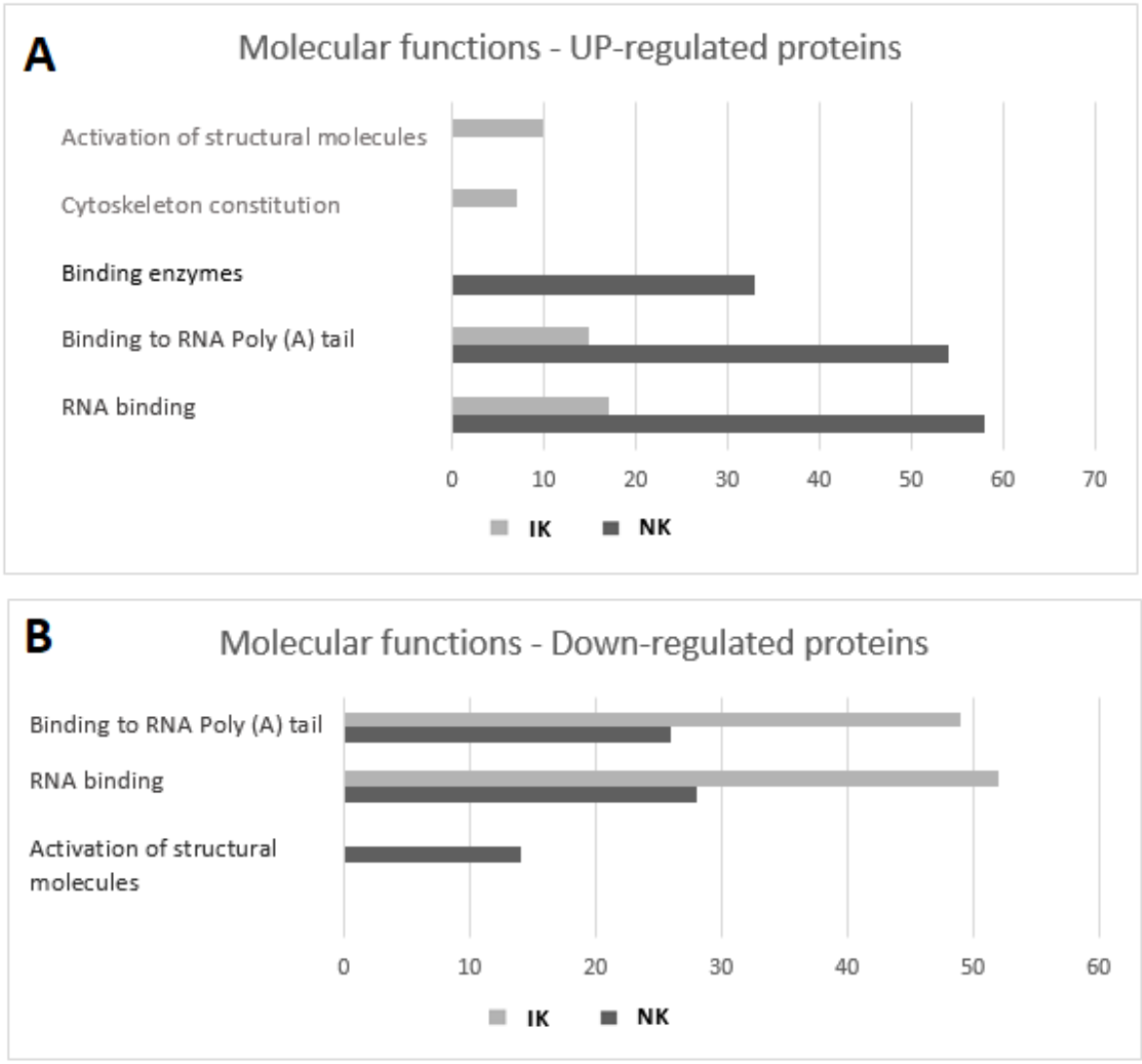

Figure 4. Quantification of up-regulated (a) and down-regulated (b) proteins related to each molecular function in normal and inverted karyotype cells. IK, inverted karyotype; NK, normal karyotype.

Protein interaction networks and measures of centrality

Regarding the protein interaction network of normal karyotype cells, the KRT16 was the bottleneck protein, meaning the articulation point in the network (Figure 5a). The centrality measurement graph shows that KRT16 is the hub protein with the highest betweenness value (Figure 5b). Regarding the protein interaction network of inverted karyotype cells, the RHOA was the bottleneck protein in the network (Figure 5c). The centrality measurement graph shows that RHOA is the protein with the highest betweenness value (hub) (Figure 5d).

Regarding the up-regulated proteins of normal karyotype cells, the GAPDH protein is the articulation point in the network (bottleneck protein) with the highest betweenness value (hub) in the centrality measurement graph (Figure 6a, 6b). Regarding the up-regulated proteins of inverted karyotype cells, the proteins with the highest betweenness-degree were CCT3 and DECR1 (Figure 6d). This result indicates that CCT3 and DECR1 are the network hubs. CCT3 and DECR1 are also the bottlenecks in the protein network (Figure 6c).

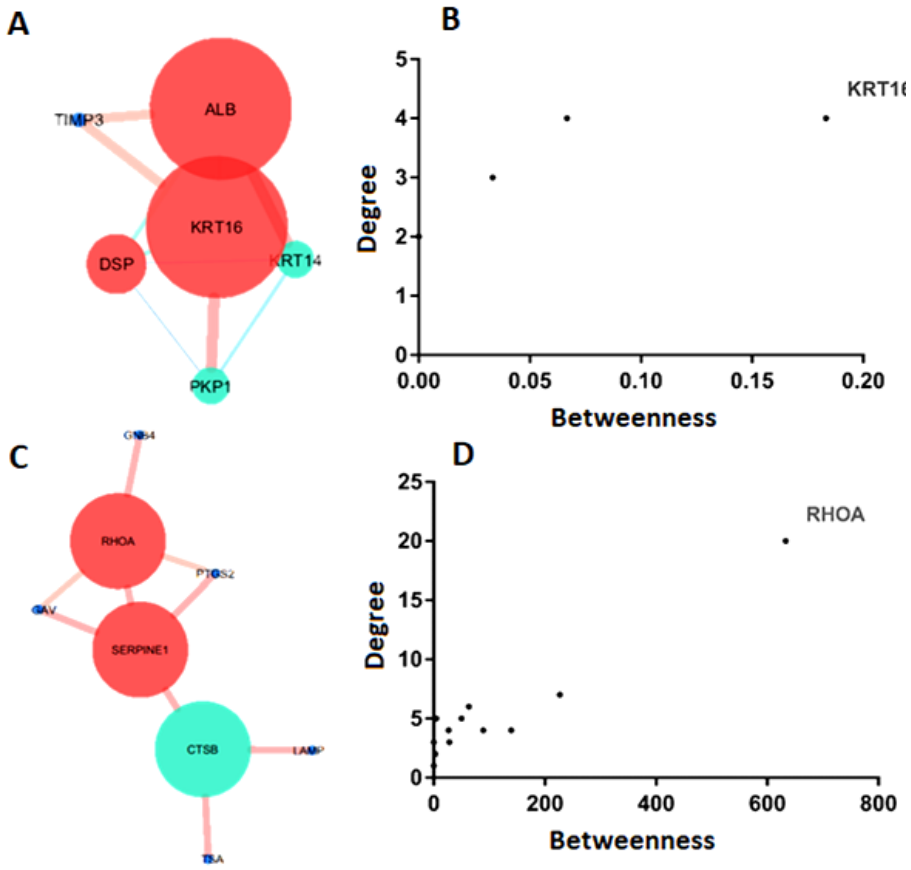

Figure 5. a. Protein interaction network of normal karyotype cells. b. Measurements of centrality of normal karyotype cell proteins. c. Protein interaction network of inverted karyotype cells. d. Measurements of centrality of inverted karyotype cell proteins. Thick bars represent strong interactions. Thin bars represent weak interactions.

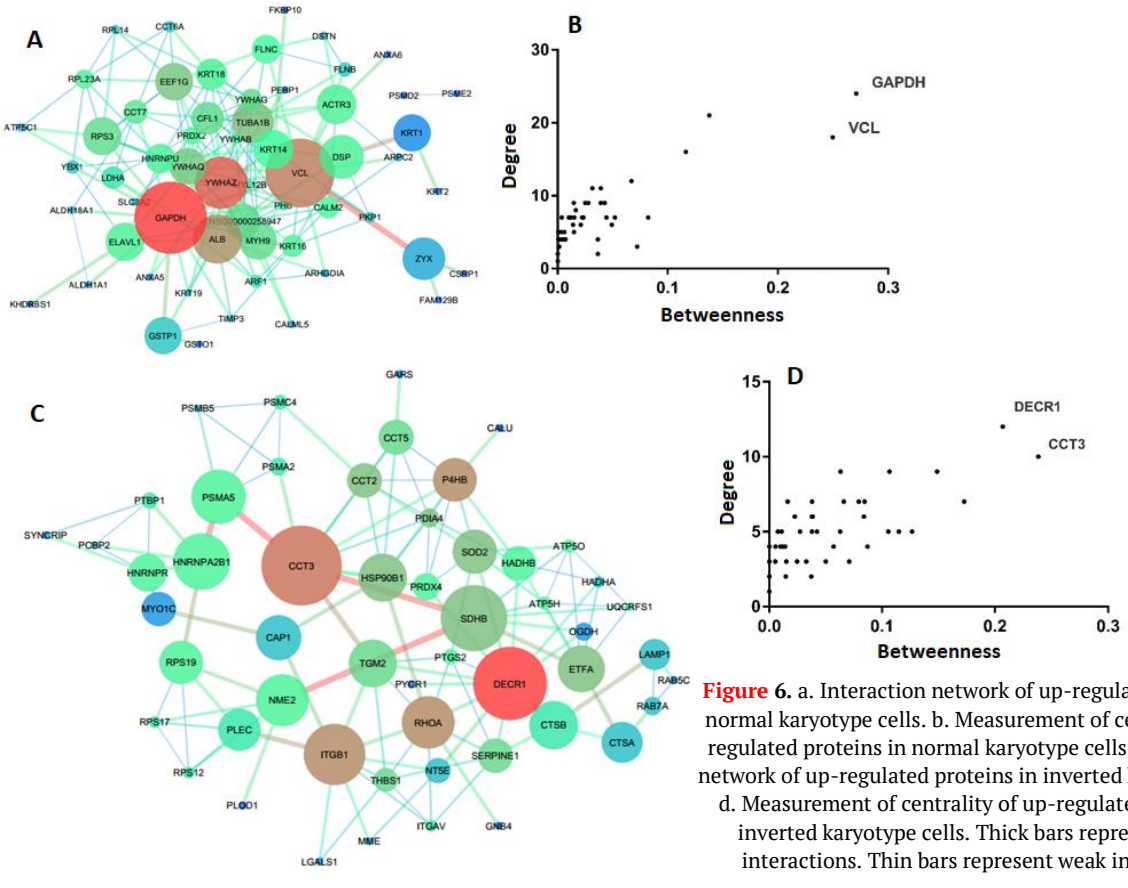

Figure 6. a. Interaction network of up-regulated proteins in normal karyotype cells. b. Measurement of centrality of up-regulated proteins in normal karyotype cells. c. Interaction network of up-regulated proteins in inverted karyotype cells. d. Measurement of centrality of up-regulated proteins in inverted karyotype cells. Thick bars represent strong interactions. Thin bars represent weak interactions.

Regarding the down-regulated proteins of normal karyotype cells, the UBC protein is clearly the bottleneck in the network, with the highest betweenness-degree value in the centrality measurement graph (Figure 7a, 7b). This result indicates that UBC is the hub. Finally, regarding the down-regulated proteins of inverted karyotype cells, the GAPDH protein was again highlighted as the bottleneck in the network, with the highest betweenness-degree value in the centrality measurement graph (Figure 7c, 7d). This result indicates that GAPDH is the hub.

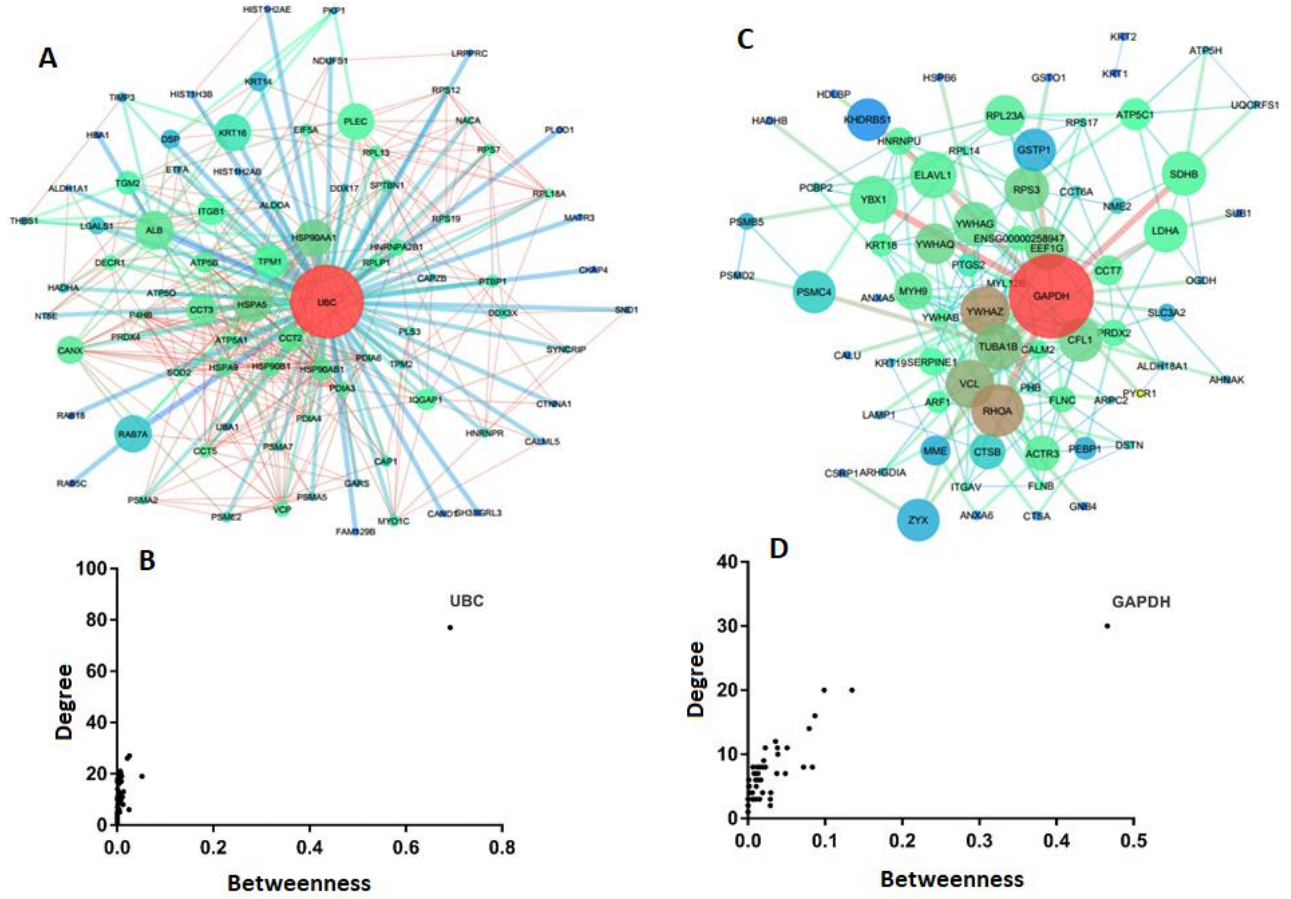

Figure 7. a. Interaction network of down-regulated proteins in normal karyotype cells. b. Measurement of centrality of down-regulated proteins in normal karyotype cells. c. Interaction network of down-regulated proteins in inverted karyotype cells. d. Measurement of centrality of down-regulated proteins in inverted karyotype cells. Thick bars represent strong interactions. Thin bars represent weak interactions.

Discussion

This paper analyzed the expression profile of human MSC with normal and inverted (inv(3)(p25p13) karyotypes and pointed out some biological processes and molecular functions of these cell proteins. Bryukhovetskiy et al. (2014) performed proteomics using cells from bone marrow and nerve tissue. They found 607 stem cell proteins from bone marrow and 1052 stem cell proteins from nerve tissue. They used two different spectrometers with different ionization sources in the experiments; this fact probably justifies a large number of proteins found, since different spectrometers have a higher resolution power (Angelucci et al., 2010).

Firstly, normal karyotype cells had more BP and MF when compared to inverted karyotype cells ($p < 0.05$) (Figure 2). The cytoskeleton organization (the main biological process found in inverted karyotype cell proteins) and the cytoskeleton constitution (the main molecular function found in inverted karyotype cell proteins) can indicate changes in gene expression required for stem cells to give origin to a different cell line. For instance, the Direct Trans-Differentiation happens when the cell changes its cytoskeleton and its protein synthesis in order to differentiate itself in another specific cell type (Monteiro, Argolo Neto, & Del Carlo, 2010).

We also found the squamous cell carcinoma antigen 1 (SCC1) in inverted karyotype cells. SCC1 was super expressed in tumors, including the tongue, esophagus, uterine cervix, and skin tumors (Liu et al., 2015). The

inverted karyotype cells may have differentiated into tumor cells due to inversion. Studies have reported chromosomal aberrations, immortalization, and malignant transformation in fresh MSC isolated from humans and rats after a considerable period of *in vitro* expansion (Duarte et al., 2012).

Regarding the normal karyotype cell proteins, the main biological process was cell transport. Proteins related to cell differentiation need to be transported to act on RNA (Tsai et al., 2015). This corroborates with the major molecular function of normal karyotype cell proteins (RNA binding). Several proteins bind to the stem cells' RNA in order to increase the protein synthesis related to cell differentiation (Kwon et al., 2013). In addition, BPs related to cell regeneration and tissue injury were found in both cell types. However, the response to oxidative stress was only found in inverted karyotype cells, suggesting that these cells undergo greater oxidative stress when compared to normal karyotype cells.

In our study it was verified thatKRT16, a keratin family member, was the bottleneck protein regarding the normal karyotype cell proteins. Keratins are subdivided into cytokeratins and capillary keratins. Keratins are intermediate filaments of proteins responsible for the structural integrity of epithelial cells (Bragulla & Homberger, 2009), however the presence of KRT16 was due to sample contamination. Therefore, albumin is the bottleneck protein, with the second highest value of betweenness. Albumin is an intracellular and secreted plasma protein involved with the intracellular transport (biological process). This protein regulates the plasma colloid osmotic pressure and acts as a carrier protein for a wide range of endogenous molecules including hormones, fatty acids, and metabolites, as well as exogenous drugs (Naveen, Akshata, Pimple, & Chaudhari, 2016).

Albumin was associated with a positive prognosis in cancer. Pretreatment with serum albumin has useful significance in cancer. Accordingly, serum albumin level could be used in clinical trials to better define the baseline risk in cancer patients. However, a critical gap for demonstrating causality is the absence of clinical trials demonstrating that raising albumin levels by intravenous infusion or by hyperalimentation decreases the excess risk of mortality in cancer. Albumin was verified as being expressed in normal karyotype cells (Gupta & Lis, 2010).

DSP protein is also highlighted in the network. DSP is found in the cytoskeleton, desmosomes, and plasma membrane. DSP is involved in the organization of the desmosomal cadherin-plakoglobin complexes into discreet plasma membrane domains and in anchoring intermediate filaments to the desmosomes (https://www.uniprot.org/uniprot/P15924). PKP 1 protein found in the nucleus and in desmosomes is also very important in the network, playing a key role in junctional plaques and contributing to epidermal morphogenesis (https://www.uniprot.org/uniprot/Q13835).

RHOA was the bottleneck protein regarding the inverted karyotype cell proteins. RHOA is a member of the GTPase family and has been reported as regulating various biological activities, including the formation of stress fibers, gene transcription, membrane transport, and cell adhesion. RHOA is also related to cell survival and cell proliferation, and can therefore be related to cancer. RHOA was in fact super-expressed in inverted karyotype cells (Li, Chen, & Xu, 2011). Although RHOA has the highest betweenness degree, Figure 5c also highlights Serpine1 and CTSB. Interestingly, Serpine1 (https://www.proteinatlas.org/ENSG00000106366-SERPINE1/tissue) and CTSB (https://www.proteinatlas.org/ENSG00000164733-CTSB/tissue) genes are both related to cancer.

The analysis of up-regulated and down-regulated proteins of normal karyotype and inverted karyotype cells, respectively, showed that the bottleneck protein of both interaction networks is GAPDH. GAPDH is an enzyme which plays an important role in glycolysis. GAPDH catalyzes the phosphorylation of glyceraldehyde-3-phosphate into 1,3-bisphosphoglycerate in glucose metabolism using nicotinamide adenine dinucleotide (NAD) as a cofactor. Experimental evidence suggests that GAPDH is actually a multifunctional protein. GAPDH can regulate gene expression/transcription, has kinase/phosphotransferase activity, facilitates vesicular transport, and interacts with molecules, including ribozymes, glutathione (GSH), p53, and nitric oxide (El Kadmiri et al., 2014).

Although GAPDH has the highest betweenness degree, Figure 6a also highlights VCL. VCL binds to actin, is associated with the membrane and is found in the cell-cell and cell-matrix junctions. VCL has the ability to assemble the actin cytoskeleton and anchor it to the cell membrane through integrins (Zemljic-Harpf et al., 2014). This ability might suggest an adhesion activity between the stem cells, with each other and with the extracellular matrix. Defects in VCL are the cause of dilated cardiomyopathy (https://www.proteinatlas.org/ENSG00000035403-VCL/tissue).

In analyzing the up-regulated proteins of inverted karyotype cells, CCT3 and DECR1 were characterized as the bottleneck proteins. CCT3 is a protein subunit included in the chaperonins group, and present in eukaryotic cells. Chaperonins use ATP hydrolysis energy to increase the efficiency of the reactions, helping other proteins reach their functional conformations. The group of chaperonins in which the CCT3 is included has roles in actin and tubulin folding. These chaperonins also regulate molecules responsible for cell division and cytoskeletal regulatory proteins (Nadler-Holly et al., 2012). The bottleneck protein DECR1 is an enzyme involved in the auxiliary pathway of fatty acid oxidation. DECR 1 limits the rate of a process which prepares polyunsaturated fatty acids to be used as substrates for beta-oxidation (Ursini-Siegel et al., 2007).

Finally, we found that UBC was the bottleneck protein among the down-regulated proteins of normal karyotype cells. Literature indicates that the UBC gene is required for extra ubiquitin synthesis during oxidative stress, and ubiquitin is able to remove damaged proteins. The loss of UBC gene function cannot be compensated by UBC gene induction. A decrease in ubiquitin levels leads to a decrease in the destruction of non-functional or defective proteins due to oxidative stress. We found low UBC expression in normal karyotype cells, and therefore we can suggest that these cells are not susceptive to high levels of oxidative stress (Crinelli et al., 2015). Overwall, these data may contribute to studies aiming toward genetic stability analyses of human MSC.

Conclusion

The results suggest that the paracentric inversion inv(3)(p25p13) induced cellular stress in human MSCh, since proteins related to stress response were super expressed in inverted karyotype cells. In addition, we found the presence of squamous cell carcinoma antigen 1, Serpine 1, RHOA, and CTSB in inverted karyotype cells. Therefore, we can suggest that the inversion can contribute to genetic instability since these proteins are related to cancer. Albumin is related to a positive prognosis in cancer, and was super-expressed in normal karyotype cells. Finally, the low Ubiquitin levels in normal karyotype cells, possibly indicating low oxidative stress in these cells.

Acknowledgements

This work was financed by the governmental Brazilian agency *Conselho Nacional de Desenvolvimento Científico e Tecnológico* (CNPq). We acknowledge CNPq and the Laboratory of Immunogenetics (Department of Biochemistry) of the *Univerisdade Federal do Rio Grande do Norte*. We also acknowledge the Mass Spectrometry Laboratory of the National Laboratory of Biosciences of the *Universidade de Campinas*.

References

Angelucci, S., Marchisio, M., Di Giuseppe, F., Pierdomenico, L., Sulpizio, M., Eleuterio, E., ... Di Ilio, C. (2010). Proteome analysis of human Wharton's jelly cells during *in vitro* expansion. *Proteome Science, 8*(18), 18. doi: 10.1186/1477-5956-8-18

Barbosa, E. B., Vidotto, A., Polachini, G. M., Henrique, T., Marqui, A. B. T., & Tajara, E. H. (2012). Proteomics: methodologies and applications to the study of human diseases. *Revista da Associação Médica Brasileira, 58*(3), 366-375. doi: 10.1016/S2255-4823(12)70209-6

Bragulla, H. H., & Homberger, D. G. (2009) Structure and functions of keratin proteins in simple, stratified, keratinized and cornified epithelia. *Journal of Anatomy, 214*(4), 516-559. doi: 10.1111/j.1469-7580.2009. 01066.x

Bryukhovetskiy, A., Shevchenko, V., Kovalev, S., Chekhonin, V., Baklaushev, V., Bryukhovetskiy, I., & Zhukova, M. (2014). To the novel paradigm of proteome-based cell therapy of tumors: through comparative proteome mapping of tumor stem cells and tissue-specific stem cells of humans. *Cell Transplantation, 23*(1), 151-170. doi: 10.3727/096368914X684907

Crinelli, R., Bianchi, M., Radici, L., Carloni, E., Giacomini, E., & Magnani, M. (2015). Molecular dissection of the human ubiquitin C promoter reveals heat shock element architectures with activating and repressive functions. *PLoS ONE, 10*(8), e0136882. doi: 10.1371/journal.pone.0136882

Dominici, M., Le Blanc, K., Mueller, I., Slaper-Cortenbach, I., Marini, F. C., Krause, D. S., ... Horwitz, E. M. (2006). Minimal criteria for defining multipotent mesenchymal stromal cells. The International Society for Cellular Therapy position statement. *Cytotherapy, 8*(4), 315-317. doi: 10.1080/14653240600855905

Duarte, D. M., Cornélio, D. A., Corado, C., Medeiros, V. K. S., Araújo, L. A. C. X., Cavalvanti, G. B., & Medeiros, S. R. B. (2012). Chromosomal characterization of cryopreserved mesenchymal stem cells from the human subendothelium umbilical cord vein. *Regenerative Medicine, 7*(2), 147-157. doi: 10.2217/rme.11.113

El Kadmiri, N., Slassi, I., El Moutawakil, B., Nadifi, S., Tadevosyan, A., Hachem, A., & Soukri, A. (2014). Glyceraldehyde-3-phosphate dehydrogenase (GAPDH) and Alzheimer's disease. *Pathologie Biologie, 62*(6), 333–336. doi: 10.1016/j.patbio.2014.08.002

Fan, C.-G., Zhang, Q.-J., & Zhou, J.-R. (2011). Therapeutic potentials of mesenchymal stem cells derived from human umbilical cord. *Stem Cell Reviews and Reports, 7*(1), 195-207. doi: 10.1007/s12015-010-9168-8

Foster, L. J., Zeemann, P. A., Li, C., Mann, M., Jensen, O. N., & Kassem, M. (2005). Differential expression profiling of membrane proteins by quantitative proteomics in a human mesenchymal stem cell line undergoing osteoblast differentiation. *Stem Cells, 23*(9), 1367-1377. doi: 10.1634/stemcells.2004-0372

Gupta, D., & Lis, C.G. (2010). Pretreatment serum albumin as a predictor of cancer survival: a systematic review of the epidemiological literature. *Nutrition Journal, 9*(69). doi: 10.1186/1475-2891-9-69

He, D., Zhang, Z., Lao, J., Meng, H., Han, L., Chen, F., ... Xu, Y. (2016). Proteomic analysis of the peri-infarct area after human umbilical cord mesenchymal stem cell transplantation in experimental stroke. *Aging and Disease, 7*(5), 623. doi: 10.14336/AD.2016.0121

Kwon, S. C., Yi, H., Eichelbaum, K., Föhr, S., Fischer, B., You, K. T., ... Kim, V. N. (2013). The RNA-binding protein repertoire of embryonic stem cells. *Nature Structural Molecular Biology, 20*(9), 1122–30. doi: 10.1038/nsmb.2638

Lee, S. K., Kim, J. H., Kim, S.-S., Kang, T., Park, N. H., Kwon, K.-H., ... Park, Y. M. (2013). Profiling and semiquantitative analysis of the cell surface proteome in human mesenchymal stem cells. *Analytical and Bioanalytical Chemistry, 405*(16), 5501-5517. doi: 10.1007/s00216-013-6969-z

Li, Y., Chen, Y., & Xu, J. (2011). Factors influencing RhoA protein distribution in the nucleus. *Molecular Medicine Reports, 4*(6), 1115–1119. doi: 10.3892/mmr.2011.556

Liu, J., Gao, Y., Yang, B., Jia, X., Zhai, D., Li, S., ... Wang, Y. (2015). Overexpression of squamous cell carcinoma antigen 1 is associated with the onset and progression of human hepatocellular carcinoma. *Archives of Medical Research, 46*(2), 133-141. doi: 10.1016/j.arcmed.2015.03.003

Mesquita, E. T., Jorge, A. J. L., Souza Junior, C. V., & Cassino, J. P. P. (2014). Systems biology applied to heart failure with normal ejection fraction. *Arquivos Brasileiros de Cardiologia, 102*(5), 510-517. doi: 10.5935/abc.20140062

Monteiro, B. S., Argolo Neto, N. M., & Del Carlo, R. J. (2010). Células-tronco mesenquimais. *Ciência Rural, 40*(1), 238–245. doi: 10.1590/S0103-84782010000100040

Nadler-Holly, M., Breker, M., Gruber, R., Azia, A., Gymrek, M., Eisenstein, M., ... Horovitz, A. (2012). Interactions of subunit CCT3 in the yeast chaperonin CCT/TRiC with Q/N-rich proteins revealed by high-throughput microscopy analysis. *PNAS - Proceedings of the National Academy of Sciences of the United States of America, 109*(46), 18833-18838. doi: 10.1073/pnas.1209277109

Naveen, R., Akshata, K., Pimple, S., & Chaudhari, P. (2016). A review on albumin as drug carrier in treating different diseases and disorders. *Der Pharmacia Sinica, 7*(1), 11-15.

Proteome Software. (2019). *Leading Edge Analytics for Mass Spectrometry* [Software]. Portland, OR: Proteome Software. Retrieved on June 15, 2019 from http://www.proteomesoftware.com/products/

Rigola, M. A., Baena, N., Català, V., Lozano, I., Gabau, E., Guitart, M., & Fuster, C. (2015). A 11.7-Mb paracentric inversion in chromosome 1q detected in prenatal diagnosis associated with familial intellectual disability. *Cytogenetic and Genome Research, 146*(2), 109-114. doi: 10.1159/000437127

Shevchenko, A., Wilm, M., Vorm, O., & Mann, M. (1996). Mass spectrometric sequencing of proteins from silver-stained polyacrylamide gels. *Analytical Chemistry, 68*(5), 850-858. doi: 10.1021/ac950914h

The human protein Atlas. (2019). CTSB. Retrieved on June 17, 2019 from https://www.proteinatlas.org/ENSG00000164733-CTSB/tissue

The human protein Atla. (2019). Serpine1. Retrieved on June 19, 2019 from https://www.proteinatlas.org/ENSG00000106366-SERPINE1/tissue

The human protein Atlas. (2019). VCL. Retrieved on June 23, 2019 from https://www.proteinatlas.org/ENSG00000035403-VCL/tissue

Tsai, E. M., Wang, Y.-C., Lee, T. T.-Y., Tsai, C.-F., Chen, H.-S., Lai, F.-J., ... Lee, J.-N. (2015). Dynamic trk and G protein signalings regulate dopaminergic neurodifferentiation in human trophoblast stem cells. *PLoS ONE, 10*(11), e0143852. doi: 10.1371/journal.pone.0143852

Uniprot. (2019). UniProtKB-P15924 (DESP_HUMAN). Retrieved on June 26, 2019 from https://www.uniprot.org/uniprot/P15924

Uniprot. (2019). UniProtKB-Q13835 (PKP1_HUMAN). Retrieved on July 1, 2019 from https://www.uniprot.org/uniprot/Q13835

Ursini-Siegel, J., Rajput, A. B., Lu, H., Sanguin-Gendreau, V., Zuo, D., Papavasiliou, V., ... Muller, W. J. (2007). Elevated expression of DecR1 impairs ErbB2/Neu-induced mammary tumor development. *Molecular and Cellular Biology, 27*(18), 6361–6371. doi: 10.1128/MCB.00686-07

Valledor, L., & Jorrín, J. (2011). Back to the basics: maximizing the information obtained by quantitative two dimensional gel electrophoresis analyses by an appropriate experimental design and statistical analyses. *Journal of Proteomics, 74*(1), 1-18. doi: 10.1016/j.jprot.2010.07.007

Vieira, S. R., & Ferrari, L. P. (2013). Investigação de alterações citogenéticas em abortos espontâneos: um retrospecto de 2006 a 2011. *Caderno da Escola de Saúde, 2*(10), 1-20.

Yun, J. W., Ahn, J. H., Kwon, E., Kim, S. H., Kim, H., Jang, J. J., ... Kang, B. C. (2016). Human umbilical cord-derived mesenchymal stem cells in acute liver injury: hepatoprotective efficacy, subchronic toxicity, tumorigenicity, and biodistribution. *Regulatory Toxicology Pharmacology, 81*, 437-447. doi: 10.1016/j.yrtph.2016.09.029

Zemljic-Harpf, A. E., Godoy, J. C., Platoshyn, O., Asfaw, E. K., Busija, A. R., Domenighetti, A. A., & Ross, R. S. (2014). Vinculin directly binds zonula occludens-1 and is essential for stabilizing connexin-43-containing gap junctions in cardiac myocytes. *Journal of Cell Science, 127*(5), 1104–16. doi: 10.1242/jcs.143743

SUPPLEMENTARY MATERIAL

Table S1. Proteins of cells with inverted karyotype. Data were generated with Scaffold software.

Protein	Accession Number	IK Spectra count[a]	NK Spectra count[b]	Fold Change[c]
Retinal Dehydrogenase 1	21361176	20	0	0
Squamous Cell Carcinoma Antigen-1	193792580	14	0	0
Keratin 16	1195531	28	0	0
Keratin 14	12803709	24	0	0
Fam129b	32425737	2	0	0
Desmoplakin I	1147813	8	0	0
Heat Shock	119582699	7	0	0
Hpa28	1008915	1	0	0
Threonine-Protein	114576744	2	0	0
Ras-Gtpase-Activating Protein	119582065	4	0	0
Pro2619	11493459	4	0	0
JUP Protein	15080189	5	0	0
Calmodulin-Like Skin Protein C Terminal Domain	109157166	5	0	0
Band-6-Protein	535015	2	0	0
Metalloproteinases-3	1304484	2	0	0

[a]IK: Inverted karyotype; [b]NK: Normal karyotype; [c]Fold Change '0' means that there were no differences in the proteins karyotypes expressions

Table S2. Proteins of cells with normal karyotype. Data were generated with Scaffold software.

Protein name	Accession Number	IK Spectra counta	NK Spectra countb	Fold Changec
NME1-NME2 Protein	66392203	0	6	0
Procathepsin B At 3.2	157833437	0	6	0
Plasminogen Activator Inhibitor 1	10835159	0	4	0
Arginine	119624305	0	3	0
Unnamed Protein Product	194388432	0	3	0
CAPNS1 Protein	15080279	0	3	0
HYOU1 Protein	116283339	0	2	0
Unnamed Protein Product	189065537	0	3	0
ATP Synthase	51479152	0	3	0
Neprilysin	116256327	0	6	0
26S Protease Regulatory Subunit 6B Isoform 2	24430155	0	3	0
Pyrroline5-Carboxylate Reductase	114794869	0	5	0
Reticulon 4	119620534	0	5	0
Tat-Associated Protein	1096067	0	3	0
Ahnak	61743954	0	6	0
40S Ribosomal Protein S17	4506693	0	4	0
Recname	143811408	0	2	0
Dihydrolipoamide S-Acetyltransferase	119587578	0	3	0
Physiological Dimer Hpp Precursor	2098347	0	3	0
Leucine	119579268	0	3	0
Ribosomal Protein L3	119580717	0	5	0
Poly(Rc)-Binding Protein	14141166	0	1	0
Unnamed Protein Product	194375834	0	3	0
Cytochrome B-C1 L	163644321	0	1	0
Glycosyltransferase	119605027	0	1	0
Cyclooxygenase2	181254	0	3	0
Hydroxyacyl-Coenzyme A Dehydrogenase	119621106	0	3	0
GDP Dissociation Inhibitor 2	119606836	0	1	0
Guanine Nucleotide-Binding Protein	11055998	0	2	0
Hcg2016877	119594653	0	1	0
Unnamed Protein Product	189065417	0	2	0
Cysteine and Glycine-Rich Protein 2	4503101	0	2	0
Proteasome	195539356	0	1	0
Hcg39912	119576757	0	1	0
Glycoprotein 1	112380628	0	2	0
Glutaminase	114582297	0	2	0
Aconitase 2	123228108	0	3	0
Unnamed Protein Product	193786545	0	2	0
Ruvb	119599729	0	1	0
SUB1 Homolog	16307067	0	1	0
Ubiquinone	115387094	0	2	0

Protein name	Accession Number	IK Spectra counta	NK Spectra countb	Fold Changec
RNA Binding Protein	119626277	0	2	0

[a]IK: Inverted karyotype; [b]NK: Normal karyotype; [c]Fold Change '0' means that there were no differences in the proteins karyotypes expressions

Table S3. Proteins of cells with inverted and normal karyotype. Data were generated with Scaffold software.

Protein name	Accession Number	IK Spectra count[a]	NK Spectra count[b]	Fold Change[c]
Ribonucleoprotein M	119589327	1	15	0.08
Procollagen-Lysine 1	16741721	1	9	0.1
Superoxide Dismutase	110590806	2	16	0.1
Rab5C	41393545	1	8	0.2
Glucosidase	119594451	5	30	0.2
Plectin	1477646	1	7	0.2
Unnamed Protein Product	158254970	1	7	0.2
Cytochrome B5	119593674	1	7	0.2
Proteasome	54696300	1	6	0.2
Rab11B	14249144	1	6	0.2
Unnamed Protein Product	194381290	8	41	0.2
Unnamed Protein Product	158255378	2	10	0.2
Ribosomal Protein L9	119613332	1	5	0.2
Transmembrane Emp24	119605373	1	5	0.2
Hmtssb	126030307	1	5	0.2
SYNCRIP Protein	116283697	2	9	0.3
Unnamed Protein Product	158261055	1	4	0.3
Prohibitin 2	119609105	2	9	0.3
Fibronectin 1	119590943	64	224	0.3
Rab7	1174149	5	16	0.3
Trifunctional Enzyme	20127408	4	12	0.3
Chaperonin Containing TCP1	14124984	4	12	0.3
Unnamed Protein Product	37138	6	20	0.3
Splicing Factor Proline	119627830	2	8	0.3
Ribosomal Protein S19	16924231	4	11	0.3
Unknown	12804225	5	14	0.4
Matrin-3	21626466	4	10	0.4
Hcg1994130	119570641	4	10	0.4
Electron Transfer Flavoprotein	189181759	2	7	0.4
Ribonucleoproteins C1 $C2^{-1}$-Like	109082737	4	10	0.4
Epb72	119578798	1	3	0.4
Peroxiredoxin 4	149243259	1	3	0.4
2,4-Dienoyl-Coa Reductase	1575000	1	3	0.4
Proteasome	4506181	1	3	0.4
Polypyrimidine	119581557	6	16	0.4
Ribonucleoproteins B1	14043072	5	13	0.4
Glycyl-Trna Synthetase	116805340	4	9	0.4
Calreticulin	119604736	10	25	0.4
Myosin-Ic	124494238	2	6	0.4
Hcg2043289	119575627	2	6	0.4
Hcg1640785	119569329	2	6	0.4
Unnamed Protein Product	158256826	8	21	0.4
Ribosomal Protein S24	119575003	6	14	0.4
Unnamed Protein Product	189054446	6	14	0.4
Hcg1745306	119606268	2	5	0.5
Proteasome	119567805	2	5	0.5
Nucleosome Structure	296863426	1	3	0.5
Signal Recognition Particle	197099116	2	5	0.5
Sh3	119628236	1	3	0.5
Transferrin Receptor	119574056	1	3	0.5
Endoplasmin Precursor	4507677	31	67	0.5
Mitochondrial Precursor	4502303	4	8	0.5
40S Ribosomal Protein S12	14277700	4	8	0.5
Unnamed Protein Product	189055102	10	20	0.5
2-Oxoglutarate 5-Dioxygenase 2	119599346	6	12	0.5
Protein Disulfide	20070125	23	45	0.5
Lamin A	119573381	38	76	0.5
Voltage-Dependent Anion Channel 2	119574954	10	19	0.5

Protein name	Accession Number	IK Spectra count[a]	NK Spectra count[b]	Fold Change[c]
Human Galectin1	42542977	28	54	0.5
X-Ray	169145200	4	7	0.5
3'-Phosphoadenosine 5'-Phosphosulfate Synthase 2	119570566	4	7	0.5
T-Plastin Polypeptide	190028	10	18	0.5
Heat Shock Protein	153792590	25	47	0.5
Ribosomal Protein	337518	6	11	0.5
Histone H2A Type 1-B E^{-1}	10645195	19	34	0.6
Ribosomal Protein S18	119624101	7	13	0.6
Chain B	157879202	5	9	0.6
Hcg2013819	119603728	2	4	0.6
Unnamed Protein Product	194380796	2	4	0.6
Far Upstream Element	119626762	2	4	0.6
Unnamed Protein Product	194375608	2	4	0.6
Tapasinerp57	220702506	26	46	0.6
Ubiquitin	23510338	11	19	0.6
Mitochondrial F1 Complex	127798841	11	19	0.6
Glucose-Regulated Protein	16507237	59	99	0.6
Initiation Factor Eif5a	183448388	4	6	0.6
Rab18	10880989	4	6	0.6
Heat Shock	12653415	26	44	0.6
ATP-Dependent RNA Helicase DDX17	148613856	5	8	0.6
Tropomyosin Beta	47519616	30	48	0.6
Unnamed Protein Product	194386896	32	51	0.6
Protein L13	15431295	6	9	0.6
Mitochondrial Precursor	32189394	48	75	0.6
Calnexin Precursor	10716563	17	26	0.7
Cytoskeleton-Associated Protein 4	19263767	38	57	0.7
Tropomyosin Alpha1	27597085	26	39	0.7
Alpha1(E)-Catenin	1172426	5	7	0.7
Phosphoprotein P1	31979223	5	7	0.7
L18a	11415026	2	3	0.7
PSMA7 Protein	116283481	4	5	0.7
Myoferlin	119570458	2	3	0.7
Fructose-Bisphosphate	119600342	1	2	0.7
Spectrin	112382250	2	3	0.7
Unnamed Protein Product	189065399	1	2	0.7
Sec23A	109083408	2	3	0.7
Unnamed Protein Product	189053683	2	3	0.7
Protein 1	141797011	1	2	0.7
Unnamed Protein Product	14042058	1	2	0.7
Hcg2028724	119601423	8	12	0.7
Hcg21078	119568094	6	9	0.7
Drebrin 1	119605395	6	9	0.7
Protein 5	1710248	29	40	0.7
Ribosomal Protein SA	119584991	8	10	0.8
Ribosomal Protein S8	119627428	12	15	0.8
Heat Shock Protein	4504517	36	44	0.8
Cyclosporin	1310882	28	33	0.8
Actin Related Protein 2 3^{-1} Complex	119618319	4	4	0.8
Hexokinase 1	119574708	7	9	0.8
Unnamed Protein Product	194382308	4	4	0.8
Glycoprotein 2	169790833	4	4	0.8
Alpha-Actinin4	12025678	108	128	0.8
Profilin I	157833469	20	24	0.9
Unnamed Protein Product	194380758	13	15	0.9
Ribosomal Protein S16	119577296	13	15	0.9
Malate Dehydrogenase	21735621	19	22	0.9
Major Vault Protein	19913410	25	29	0.9
Alpha-Actinin1	194097350	160	184	0.9
Non-Erythrocytic 1	119608213	6	7	0.9
Ribosomal Protein L30	119612175	8	9	0.9
Ribosomal Protein SA	119584991	8	10	0.8
Ribosomal Protein S8	119627428	12	15	0.8
Heat Shock Protein	4504517	36	44	0.8
Cyclosporin	1310882	28	33	0.8

Protein name	Accession Number	IK Spectra count[a]	NK Spectra count[b]	Fold Change[c]
Actin Related Protein 2 3^{-1} Complex	119618319	4	4	0.8
Hexokinase 1	119574708	7	9	0.8
Unnamed Protein Product	194382308	4	4	0.8
Glycoprotein 2	169790833	4	4	0.8
Alpha-Actinin4	12025678	108	128	0.8
Profilin I	157833469	20	24	0.9
Unnamed Protein Product	194380758	13	15	0.9
Ribosomal Protein S16	119577296	13	15	0.9
Malate Dehydrogenase	21735621	19	22	0.9
Major Vault Protein	19913410	25	29	0.9
Alpha-Actinin1	194097350	160	184	0.9
Non-Erythrocytic 1	119608213	6	7	0.9
Ribosomal Protein L30	119612175	8	9	0.9
Unnamed Protein Product	194382308	4	4	0.8
Glycoprotein 2	169790833	4	4	0.8
Alpha-Actinin4	12025678	108	128	0.8
Profilin I	157833469	20	24	0.9
Unnamed Protein Product	194380758	13	15	0.9
Ribosomal Protein S16	119577296	13	15	0.9
Malate Dehydrogenase	21735621	19	22	0.9
Major Vault Protein	19913410	25	29	0.9
Alpha-Actinin1	194097350	160	184	0.9
Non-Erythrocytic 1	119608213	6	7	0.9
Ribosomal Protein L30	119612175	8	9	0.9
Unnamed Protein Product	194382308	4	4	0.8
Glycoprotein 2	169790833	4	4	0.8
Alpha-Actinin4	12025678	108	128	0.8
Profilin I	157833469	20	24	0.9
Unnamed Protein Product	194380758	13	15	0.9
Ribosomal Protein S16	119577296	13	15	0.9
Malate Dehydrogenase	21735621	19	22	0.9
Major Vault Protein	19913410	25	29	0.9
Alpha-Actinin1	194097350	160	184	0.9
Non-Erythrocytic 1	119608213	6	7	0.9
Ribosomal Protein L30	119612175	8	9	0.9
Unnamed Protein Product	158254664	122	137	0.9
Rab1a	119620329	19	21	0.9
Heat Shock Cognate	5729877	88	95	0.9
Histone 1	119575932	35	38	0.9
Nucleophosmin	10835063	19	21	0.9
Peroxiredoxin6	4758638	12	13	0.9
Ribosomal Protein L18	119572744	10	10	0.9
40S Ribosomal Protein S14	5032051	2	3	0.9
WD Repeat Domain 1	119613093	2	3	0.9
Strongylocentrotus Purpuratus	119607750	2	3	0.9
EIF3A Protein	116283747	2	3	0.9
Unnamed Protein Product	193783525	2	3	0.9
Unnamed Protein Product	31092	34	36	0.9
Vdac1	198443050	17	18	0.9
60S Acidic Ribosomal Protein P2	4506671	14	15	0.9
40S Ribosomal Protein S9	14141193	7	8	0.9
Dehydrogenase	13786847	7	8	0.9
MYL6 Protein	113812151	23	24	1
60S Ribosomal Protein L12	4506597	13	14	1
Serpin H1 Precursor	32454741	53	54	1
40S Ribosomal Protein	114647215	8	9	1
Hcg1983058	119619436	8	9	1
Rap-Rapgap	169791854	6	6	1
Rab2A	336391093	6	6	1
Triosephosphate Isomerase 1	17389815	18	18	1
Ribonucleoprotein A1	14043070	18	18	1
Ribonucleoprotein K	119583080	16	15	1
Ribosomal Protein S10	119624187	10	9	1
Pyruvate Kinase	119598292	46	45	1
ADP-Ribosylation Factor 4	4502205	13	13	1

Protein name	Accession Number	IK Spectra count[a]	NK Spectra count[b]	Fold Change[c]
Ribosomal Protein S5	119592989	13	13	1
Hsp70 Atpase	166007012	13	13	1
Actin	4501887	275	267	1
Elongation Factor 2	4503483	83	81	1
Histone H2B	10800138	59	57	1
Tubulin Beta6	27754056	61	58	1.1
Serpin H1 Precursor	32454741	53	54	1
40S Ribosomal Protein	114647215	8	9	1
Hcg1983058	119619436	8	9	1
Rap-Rapgap	169791854	6	6	1
Rab2A	336391093	6	6	1
Triosephosphate Isomerase 1	17389815	18	18	1
Ribonucleoprotein A1	14043070	18	18	1
Ribonucleoprotein K	119583080	16	15	1
Ribosomal Protein S10	119624187	10	9	1
Pyruvate Kinase	119598292	46	45	1
ADP-Ribosylation Factor 4	4502205	13	13	1
Ribosomal Protein S5	119592989	13	13	1
Hsp70 Atpase	166007012	13	13	1
Actin	4501887	275	267	1
Elongation Factor 2	4503483	83	81	1
Histone H2B	10800138	59	57	1
Tubulin Beta6	27754056	61	58	1.1
Protein-Disulfide	192987144	4	3	1.1
Adaptor-Related Protein Complex 1	119580203	4	3	1.1
Histone H2B	10800140	60	57	1.1
Ran-Like	109099257	8	8	1.1
Tubulin	119608775	114	105	1.1
Importin	119615215	18	16	1.1
Beta-Tubulin	1297274	88	79	1.1
Phosphoglycerate Mutase 1	297302419	5	4	1.1
Filamin-B	105990514	30	27	1.1
Keratin 8	119617057	108	93	1.2
Tubulin	18088719	140	121	1.2
Glyceraldehyde-3-Phosphate Dehydrogenase	31645	78	67	1.2
Vinculin	24657579	30	26	1.2
Ribonucleoprotein U	14141161	12	10	1.2
T-Complex Protein 1	261399877	6	5	1.2
Chaperonin	119620390	6	5	1.2
Calelectrin	179976	49	41	1.2
Myosin	15809016	26	21	1.2
Chain A	157831404	62	51	1.2
Translocon-Associated Protein Subunit Delta Isoform 1 Precursor	325301072	11	9	1.3
Keratin. Type I Cytoskeletal 19	24234699	23	18	1.3
Adp-Ribosylation Factor 1	1065361	12	9	1.3
G Protein	119574079	36	28	1.3
Moesin.	119625804	25	20	1.3
14-3-3 Protein Epsilon	114665591	42	33	1.3
Unnamed Protein Product	193786502	90	69	1.3
Cofilin1	5031635	44	33	1.3
KIAA1027 Protein	20521736	68	51	1.3
Keratin 18	12653819	24	18	1.3
Glutathione Transferase P11	11514451	22	15	1.4
Ribosomal Protein L23a	119571516	11	8	1.4
Ubiquitin Thiolesterase	119613388	10	7	1.4
Hcg37214	119622042	10	7	1.4
Zyxin	119572233	7	5	1.4
Cytoplasmic 1	119612225	5	3	1.4
Chain A	157831404	62	51	1.2
Translocon-Associated Protein Subunit Delta Isoform 1 Precursor	325301072	11	9	1.3
Keratin. Type I Cytoskeletal 19	24234699	23	18	1.3
Adp-Ribosylation Factor 1	1065361	12	9	1.3
G Protein	119574079	36	28	1.3
Moesin.	119625804	25	20	1.3
14-3-3 Protein Epsilon	114665591	42	33	1.3

Protein name	Accession Number	IK Spectra count[a]	NK Spectra count[b]	Fold Change[c]
Unnamed Protein Product	193786502	90	69	1.3
Cofilin1	5031635	44	33	1.3
KIAA1027 Protein	20521736	68	51	1.3
Keratin 18	12653819	24	18	1.3
Glutathione Transferase P11	11514451	22	15	1.4
Ribosomal Protein L23a	119571516	11	8	1.4
Ubiquitin Thiolesterase	119613388	10	7	1.4
Hcg37214	119622042	10	7	1.4
Zyxin	119572233	7	5	1.4
Cytoplasmic 1	119612225	5	3	1.4
Hcg33299	119597983	2	2	1.4
Hcg1985370	119610462	1	1	1.4
Unnamed Protein Product	221045376	4	3	1.4
Ribosomal Protein L10	119593144	1	1	1.4
Kh	119627980	1	1	1.4
C-Type Mannose Receptor 2	110624774	4	3	1.4
Eukaryotic Translation Elongation Factor 1 Gamma	15530265	5	3	1.4
Flavoprotein	119571367	2	2	1.4
Coactosin-Like Protein	21624607	2	2	1.4
ATP Synthase	16877071	4	3	1.4
Protein B	181486	1	1	1.4
26S Proteasome Subunit P97	1060888	1	1	1.4
Integrin Beta 4 Binding Protein	119596626	1	1	1.4
Ribonucleoprotein H1	119574194	8	6	1.4
Pyrroline 5-Carboxylate Synthetase	1304314	6	4	1.4
Phosphorylation Independent Interactions Between 14-3-3	161172138	62	43	1.5
Ribosomal Protein S4	119592221	18	12	1.5
Unnamed Protein Product	194390460	14	9	1.5
Tsa	1617118	13	9	1.5
Myosin-9	12667788	207	134	1.5
Tyrosine 3-Monooxygenase	54696890	38	25	1.5
Chloride Intracellular Channel Protein 1	14251209	12	8	1.6
Tubulin Alpha1a	6755901	84	54	1.6
14-3-3 Protein Beta Alpha^{-1}	4507949	24	15	1.6
Prohibitin	46360168	11	7	1.6
L-Lactate Dehydrogenase	13786849	10	6	1.6
Annexin A2	18645167	139	87	1.6
Transgelin	119587704	136	81	1.7
Clathrin	119614801	7	4	1.7
Unnamed Protein Product	189053923	7	4	1.7
Calcium-Calmodulin	16974825	11	6	1.8
Unnamed Protein Product	193785841	31	17	1.8
Peroxiredoxin 1	119627382	25	14	1.8
Keratin 9	119581148	14	8	1.9
Filamin-C	116805322	50	26	2
Transgelin2-Like	297663020	64	32	2
Hcg1783090	119582155	22	10	2.1
Unnamed Protein Product	194387966	4	2	2.1
Unnamed Protein Product	10438296	4	2	2.1
Phosphatidylinositol Binding Clathrin Assembly Protein	119595524	4	2	2.1
Annexin A1	119582950	56	25	2.3
Rhogdi K113a	14278162	6	3	2.3
Unknown	13097759	25	10	2.5
Keratin	47132620	56	21	2.7
Unnamed Protein Product	189054048	7	3	2.8
Unknown	1531594	7	3	2.8
Similar To Cysteine And Glycine-Rich Protein 1	13279065	7	3	2.8
Proteasome	8394076	2	1	2.8
Hur RNA Binding Protein	1022961	8	3	3.3
Keratin 1	11935049	192	54	3.6
Ribosomal Protein L14	17932938	10	3	3.7
Recname	1703319	5	1	5.6
Hcg1995701	119584408	7	1	8.4
Ed4f2hc	145579147	7	1	8.4
RAN Binding Protein 5	119629383	7	1	8.4

Protein name	Accession Number	IK Spectra count[a]	NK Spectra count[b]	Fold Change[c]
Keratin 10	119581085	161	11	14
Filamin-C	116805322	50	26	2
Transgelin2-Like	297663020	64	32	2
Hcg1783090	119582155	22	10	2.1

[a]IK: Inverted karyotype; [b]NK: Normal karyotype; [c]Fold Change '0' means that there were no differences in the proteins karyotypes expressions.